

LONGSHORE PATTERNS OF THE SEA BOTTOM MORPHOLOGY

Giovanna Vittori¹, Huib de Swart², Paolo Blondeaux³

Abstract

It is shown that the two-dimensional flow field and the bottom configuration induced by a wave of small amplitude normally approaching a straight beach may be unstable with respect to infinitesimal perturbations. The time development of the bottom perturbation leads to the formation of crescentic forms periodic in the longshore direction. The growth of the perturbation is due to a positive feedback mechanism, involving the incoming wave, synchronous edge waves and the bedforms. In particular the growth is related to the presence of steady currents caused by the interaction of the incoming wave with synchronous edge waves which in turn are excited by the incoming wave moving over the wavy bed. For natural beaches the model predicts two maxima in the amplification rate; the former is related to incoming waves of low-frequency, the latter to wind waves. Thus two bedforms of different wavelengths can co-exist in the nearshore region, the longshore spacing of which is few hundreds and few decades of metres respectively. To illustrate the potential validity of the model, its results are compared with field data.

1 INTRODUCTION

Field surveys of the morphology of the coastal region show the existence of periodic longshore patterns. These patterns are characterized by different length scales in the range between 1 meter to 1 kilometer. Previous studies on the process originating these coastal forms assume that edge waves are the driving mechanism. However in these models bottom topography does not enter in the mechanism originating bottom forms since the dynamics of the sea bottom is not considered and sediment motion is assumed to be passively driven by the water flow.

Recently Vittori et al. (1998) have shown that rhythmic longshore patterns may be due to a feedback between water flow and the erodible bottom. In their paper it is demonstrated that crescentic forms in the coastal area, far away from the breaker line, can be produced by the time development of

¹Assistant Professor, Hydraulic Institute, University of Genoa, via Montallegro, 1 - 16145 Genova, Italy

²Professor, Institute for Marine and Atmospheric Research, Utrecht University, P.O. Box 80.005, 35 TA Utrecht, The Netherlands

³Professor, Hydraulic Institute, University of Genoa, Via Montallegro, 1 - 16145 Genoa, Italy

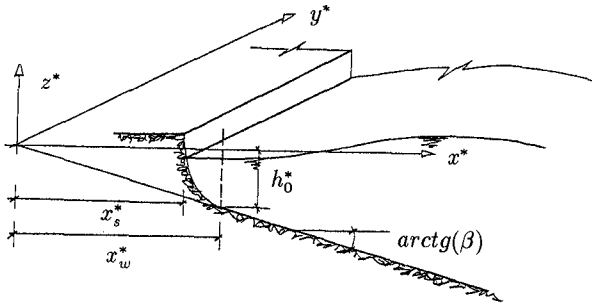


Figure 1: Sketch of the beach geometry.

small random perturbations both of the sea bottom and of the water motion which interact with a monochromatic wave which approaches the beach. The basic mechanism is that the incoming wave interacts with a small bottom perturbation (periodic in the longshore direction) and produces a synchronous edge wave. This wave subsequently interacts with the incoming wave and leads to the generation of steady currents. These currents induce a net sediment transport, the convergence pattern of which is in phase with the bedforms. Hence there is a positive feedback between the water motion and the erodible bottom which gives rise to an exponential growth of both the free surface and bottom morphology perturbations.

In the present paper the analysis of Vittori et al. (1998) is briefly outlined and their results are summarized. Then a comparison is performed between their theoretical results and field data. In particular the observations of Homma & Sonu (1963) and Pruszek et al. (1997) are considered.

2 THE THEORETICAL MODEL

In the theoretical model of Vittori et al. (1998) a simplified beach profile is used (see figure 1) which consists of two regions. In the outer region ($x^* > x_w^*$) the local water depth increases in the offshore direction with a constant slope β , starting from a finite value h_0^* at $x^* = x_w^*$. The inner region ($x_s^* < x^* < x_w^*$) is characterized by a slope which rapidly increases when moving towards the beach. The variables (x^*, y^*, z^*) denote an orthogonal coordinate system with the x^* and y^* axes lying on the still water level. The x^* -axis points offshore, while the y^* -axis is parallel to the straight beach and the z^* -axis is vertical.

The water motion in the outer region is described by the shallow water

equations which read

$$\frac{\partial(h^* + \eta^*)}{\partial t^*} + \frac{\partial[h^* + \eta^*)u^*]}{\partial x^*} + \frac{\partial[(h^* + \eta^*)v^*]}{\partial y^*} = 0 \quad (1)$$

$$\frac{\partial u^*}{\partial t^*} + u^* \frac{\partial u^*}{\partial x^*} + v^* \frac{\partial u^*}{\partial y^*} = -g^* \frac{\partial \eta^*}{\partial x^*} \quad (2)$$

$$\frac{\partial v^*}{\partial t^*} + u^* \frac{\partial v^*}{\partial x^*} + v^* \frac{\partial v^*}{\partial y^*} = -g^* \frac{\partial \eta^*}{\partial y^*} \quad (3)$$

The forcing is due to a prescribed surface gravity wave which normally approaches the straight beach and is partially reflected. This yields the matching condition (see Mei, 1989)

$$\lim_{x^* \rightarrow \infty} \eta^* = \lim_{h^* \rightarrow 0} \frac{a_x^*(x)}{2} \left[\exp(i \int \ell^* dx^*) + \hat{K} \exp(-i \int \ell^* dx^*) \right] e^{i\omega^* t^*} + c.c. \quad (4)$$

In (1), (4) h^* is the water depth, η^* is the water surface displacement, (u^*, v^*) are the depth-averaged velocity components in the cross- and long-shore directions respectively. Furthermore a_x^* , ℓ^* and ω^* are the amplitude, the wavenumber and the angular frequency of the incoming wave and \hat{K} is the complex reflection coefficient of the beach. Finally c.c. denotes the complex conjugate of a complex quantity.

By assuming that $x_w^* - x_s^*$ is much smaller than the horizontal length scale of the problem, the dynamics of the flow in the inner region is neglected and all the phenomena which take place between x_s^* and x_w^* are described by means of an appropriate boundary condition at x_w^* :

$$u^*(h^* + \eta^*) = \chi^* \eta^* \quad (5)$$

Relationship (5) simply forces a mass balance within the inner region and the constant χ^* depends on the reflection coefficient of the beach and the characteristics of the wave.

The problem is then closed by Exner equation, which forces the sediment balance, and by a constitutive relationship relating the sediment transport rate per unit width (q_x^* , q_y^*) and the water motion

$$\frac{\partial h^*}{\partial t^*} = \frac{1}{(1-p)} \left[\frac{\partial q_x^*}{\partial x^*} + \frac{\partial q_y^*}{\partial y^*} \right] \quad (6)$$

$$(q_x^*, q_y^*) = h_0^* \bar{Q} \alpha(x) (\bar{u}^*, \bar{v}^*) \quad \alpha = \overline{|u_w^* / \sqrt{g^* h_0^*}|^{b-1}} \quad (7)$$

In (5), (6) p is sediment porosity, an overbar denotes the time average over a wave cycle, α is a wave stirring coefficient which depends on the dimensionless

periodic component $u_w^*/\sqrt{g^*h_0^*}$ of the wave field, \tilde{Q} is a dimensionless constant which depends on sediment characteristics and b is assumed to be equal to 4.

The basic wave field, which is uniform in the longshore direction, can be easily determined by expanding the solution in terms of the small parameter $a = a^*/h_0^*$ (a^* denotes the wave amplitude at $x^* = x_w^*$)

$$u = \frac{u^*}{\sqrt{g^*h_0^*}} = aU_1 + O(a^2) \tag{8}$$

$$\eta = \frac{\eta^*}{h_0^*} = aE_1 + O(a^2) \tag{9}$$

$$h = \frac{h^*}{h_0^*} = \frac{x}{x_w} + O(a^2) \tag{10}$$

In (10) x is the dimensionless cross-shore coordinate ($x = x^*\omega^*/\sqrt{gh_0^*}$) and $x_w = x_w^*\omega^*/\sqrt{gh_0^*}$ is a dimensionless frequency parameter. Moreover because of the matching (4) with the deep water solution, the wave amplitude a^* is related to the wave amplitude a_∞^* of the incoming wave far from the coast ($a^* = a_\infty^*\sqrt{2\pi/\beta}$). Both the dimensionless free surface E_1 and the velocity U_1 turn out to be periodic in time with angular frequency ω^* and characterized by a cross-shore structure described by Hankel functions.

$$E_1(x, t) = \frac{1}{2} \{ H_0^{(1)}(2\sqrt{xx_w}) + \hat{K} H_0^{(2)}(2\sqrt{xx_w}) \} e^{it} + c.c. \tag{11}$$

$$U_1(x, t) = \frac{i}{2} \sqrt{\frac{x_w}{x}} \{ H_1^{(1)}(2\sqrt{xx_w}) + \hat{K} H_1^{(2)}(2\sqrt{xx_w}) \} e^{it} + c.c. \tag{12}$$

where $t = \omega^*t^*$ is the dimensionless time.

Then small perturbations of the free surface and of the bottom configuration are considered

$$\frac{\eta^*}{h_0^*} = aE_1 + \epsilon \{ A^\pm(\tau)\hat{\eta}_0(x)e^{i(k^*y^* \pm \sigma^*t^*)} + c.c. + O(a) \} \tag{13}$$

$$\frac{h^*}{h_0^*} = \frac{x}{x_w} + \epsilon \{ B^\pm(\tau)\hat{h}_0^\pm(x)e^{ik^*y^*} + c.c. + O(a) \} \tag{14}$$

where ϵ is a parameter much smaller than one (strictly infinitesimal) and τ a slow time scale defined by $\tau = a\omega^*t^*$. Of course perturbations of similar form are induced in the velocity field.

At order ϵ equations (1), (3) provide the structure of $\hat{\eta}_0(x)$

$$\hat{\eta}_0(x) = e^{-k^*x^*} U(d, 1, 2k^*x^*) \tag{15}$$

where d is equal to $(k^* - \sigma^{*2}x_w^*/(g^*h_0^*))/2k^*$ and U indicates one of the Kummer functions (Abramowitz & Stegun, 1964). Then the boundary condition (5)

yields the dispersion relation

$$d = -\frac{U(d, 1, 2k^*x_w^*)}{2U(d+1, 2, 2k^*x_w^*)} \quad (16)$$

which shows that different modes are possible. Moreover at order ϵ , $\hat{h}_0^\pm(x)$ turns out to be arbitrary as well as $A^\pm(\tau)$ and $B^\pm(\tau)$.

In order to determine \hat{h}_0^\pm and the time behaviour of A^\pm and B^\pm , it is necessary to study the interaction between the perturbations and the incoming wave which is described by the problem at order ϵa . In nonresonant cases a solution of the problem forced by the interactions of the perturbation with the basic wave field can be found and it gives rise to a slight modification of the original perturbation. However, as discussed by Guza & Davis (1974) who considered only perturbations in the water motion, many resonant cases exist and in particular resonance is present when the interaction between subharmonic edge waves (frequency σ^* equal to $\omega^*/2$) and the incoming wave is considered.

When bottom perturbations are included, it can be seen that their presence induces extra forcing terms. These terms can give rise to a secular growth of the solution if h^* is characterized by a periodic longshore dependence characterized by a wavenumber k^* equal to that of a synchronous edge wave.

In order to prevent the solution from growing unbounded on the fast time scale, a solvability condition must be imposed which leads to

$$\frac{dA^\pm}{d\tau} = \gamma_1^\pm B^+ + \gamma_2^\pm B^- \quad (17)$$

where the coefficients $\gamma_1^\pm, \gamma_2^\pm$ depend on the characteristics of the incoming wave. These equations describe the growth of the amplitude of synchronous edge waves due to their interaction with the incoming wave propagating on a wavy bottom. A further link between A^\pm and B^\pm is found by considering the bottom time development forced by the steady part of the $O(\epsilon a)$ flow. This is because the interaction of synchronous edge waves with the incoming wave generates steady currents, which cause the movement of sediment and thereby result in the formation of bedforms. Sediment continuity equation and the sediment transport rate relationship yield

$$\hat{h}_0^\pm(x) = \frac{d}{dx} \left[\overline{|U_1|^{b-1} u_1^\pm} \right] + ik \overline{|U_1|^{b-1} v_1^\pm} \quad (18)$$

$$\frac{dB^\pm}{d\tau} = Q A^\pm \quad (19)$$

where the steady velocity field described by u_1^\pm, v_1^\pm can be derived by means of the variation of the parameter method and the constant Q , which turns out to be $\hat{Q} a^{b-1}/(1-p)$, is much smaller than one.

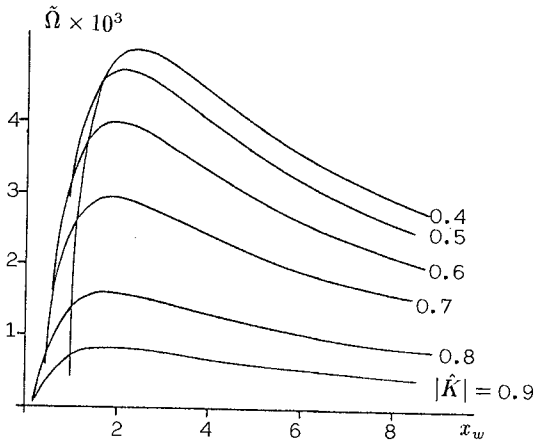


Figure 2: Maximum value of the growth rate $\tilde{\Omega}$ plotted versus x_w for different values of $|\hat{K}|$ and $n = 1$.

The solution of the amplitude equations is of exponential type

$$B^\pm \sim \exp(a^{(b+1)/2} \tilde{\Omega} \tilde{t}) \tag{20}$$

where

$$\tilde{t} = t^* \sqrt{\frac{\tilde{Q} g h_0^*}{(1-p)(x_w^*)^2}} \tag{21}$$

is a dimensionless time coordinate obtained using a morphodynamic time scale which does not depend on wave characteristics. Of course the amplification rate $\tilde{\Omega}$ appearing in (20) depends on the parameters of the problem, i.e. $x_w = x_w^* \omega^* / \sqrt{g h_0^*}$ and \hat{K} .

3 THE RESULTS

The theoretical analysis, briefly summarized in the previous section, shows that crescentic forms may appear when A and B tend to grow. Figure 2 shows the maximum value of amplification rate $\tilde{\Omega}$ versus the frequency parameter x_w for different values of $|\hat{K}|$ and for the first mode ($n = 1$). Note that $|\hat{K}|$ indicates the modulus of the reflection coefficient of the beach and its phase ϑ is determined by means of the simple model described in (Vittori & al., 1998). The results indicate that bedforms periodic in the longshore direction tend to form when the incoming wave has an angular frequency ω^* such that x_w takes values close to 4.5. However the first mode is not always the most unstable as

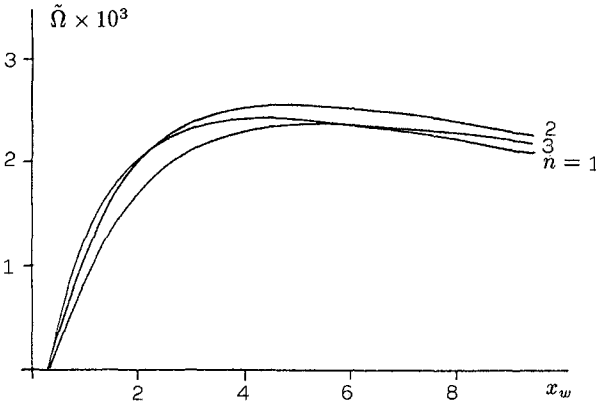


Figure 3: Maximum value of the growth rate $\tilde{\Omega}$ plotted versus x_w for different mode numbers n and $|\hat{K}| = 0.8$.

it can be seen from figure 3, where $\tilde{\Omega}$ is plotted versus x_w for $|\hat{K}| = 0.8$ and different mode numbers. In this case the second mode is the most unstable and crescentic forms appear when forced by incoming waves characterized by an angular frequency such that $x_w \cong 4.75$. By considering the behaviour of $\tilde{\Omega}$ for different values of n , x_w and \hat{K} it is possible to single out the most unstable conditions, i.e. to evaluate the frequency ω^* of the incoming wave triggering the instability of the bottom configuration and the wavelength of the most unstable mode.

Let us now compare the theoretical findings with some field data. First of all this requires the determination of the values of x_w^* and h_0^* which are representative for the actual beach profiles. Figure 4 shows one of the bottom

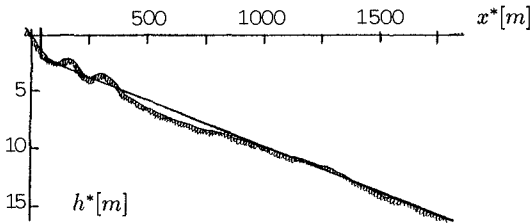


Figure 4: Bottom profile measured along Niigata beach in 1958 (Hom-ma & Sonu, 1963) and the model beach geometry.

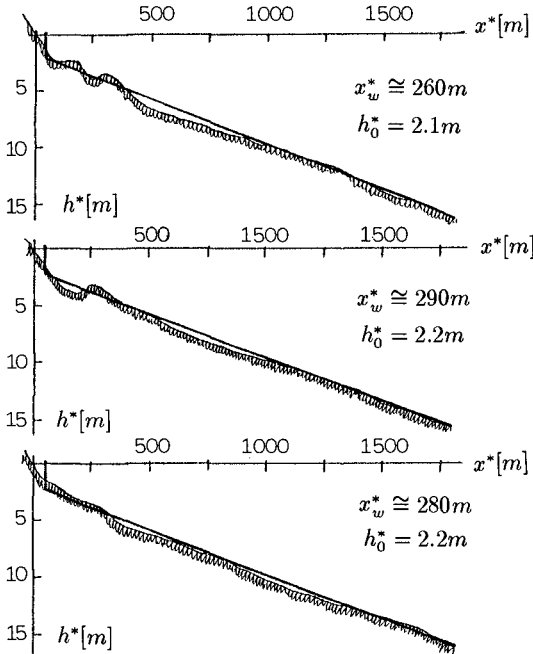


Figure 5: Bottom profiles measured along Niigata beach in 1958 (Hom-ma & Sonu, 1963) at different longshore locations along with the model beach geometry.

profiles measured by Hom-ma & Sonu (1963) at Niigata beach during 1958 along with our simplified beach profile in such a way that the differences between the two geometries are minimized in a least square sense. In this case our best fitting procedure yields $x_w^* = 260$ m and $h_0^* = 2.1$ m. However it turns out that x_w^* and h_0^* depend on the longshore coordinate as it follows from figure 5 where the beach profiles detected at different longshore locations along the Niigata coast during 1958 are shown together with the values of x_w^* and h_0^* . Hence in order to apply the theory, it is necessary to average x_w^* and h_0^* along the longshore coordinate. The data described in the paper by Hom-ma & Sonu (1963) provide the beach profiles at Niigata site at 6 longshore locations only and the average values of x_w^* and h_0^* can be determined with some uncertainty. It turns out that x_w^* and h_0^* fall within a small range around 280 m and 2.2 m respectively. The same procedure applied to the data obtained by Hom-ma & Sonu (1963) in August 1957 at Tokai beach provides values of x_w^* and h_0^* which are somewhat larger, i.e. 310 m and 2.9 m respectively. However it is necessary to point out that different wave climates make x_w^* and h_0^* to change. Indeed

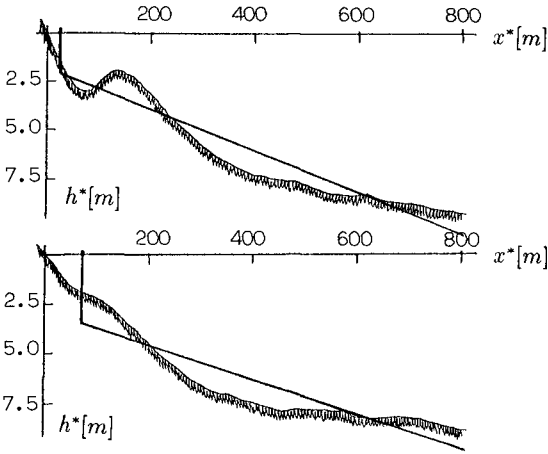


Figure 6: Bottom profiles measured along Tokai beach (Hom-ma & Sonu, 1963) along with the model beach geometry. (a) December 1956, (b) August 1957.

figure 6 shows that beach profiles detected at the same longshore location but at different times are characterized by large differences. The changes observed in the values of x_w^* and h_0^* are significant and hence the theoretical analysis should be used to indicate the range of wavelengths of possible crescentic forms rather than to predict an exact value.

Because the maximum value of the amplification rate $\tilde{\Omega}$ is around $x_w = 4.75$, the incoming waves which are most likely to give rise to the appearance of crescentic forms are those characterized by a period equal to about 80 s and 85 s for the Niigata and Tokai sites, respectively. Then the dispersion relation yields a value of the longshore wavelength of the bottom forms. For Niigata site the predicted length is around 600 m while for Tokai beach it appears that the most unstable crescentic forms are characterized by a wavelength of about 700 m. If a comparison is performed with the observed values a fair agreement is found taking into account that, at this stage, the analysis is linear and that a highly idealized model has been used. From figure 7, which shows bottom morphology measured in front of Niigata beach in 1958, it can be seen that bottom forms periodic in the longshore direction are present, which have wavelengths larger than 500 m. Likewise figure 8 clearly shows a longshore periodic pattern in the offshore bar at Tokai beach, with a wavelength which ranges between 1000 and 1500 m depending on the wave climate. The field surveys show also the presence of much shorter crescentic forms, with wavelengths of about 50 m. These bottom forms are also predicted by the theory since the total

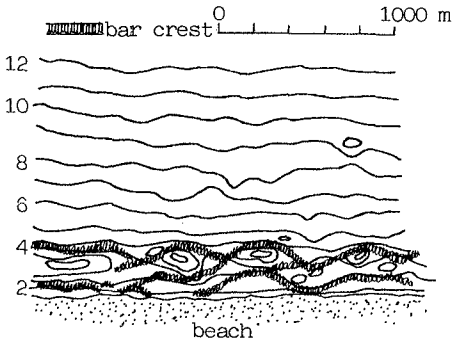


Figure 7: Bottom topography showing bar position in 1958 at Niigata beach (adapted from Hom-ma & Sonu, 1963).

amplification rate of the bottom perturbations (see (20)) is characterized by two maxima. The former is due to the maximum of $\tilde{\Omega}$, the latter is caused by maximum of the amplitude a of the incoming wave which of course depends on the frequency parameter x_w . The prediction of the smaller bottom forms would require accurate measurements of the spectrum of the incoming wave field outside the breaker zone. These data are not available for Niigata and Tokai beaches. However it can be certainly assumed that the wave spectrum is characterized by a maximum for wind waves which have periods around 10 s. With these data, the theory predicts bedforms with a longshore wavelength of about 50 m, a value which is very close to the observed one. Good agreement is also found when comparing the theoretical findings with the field survey performed at Lubiatowa (Poland) by Pruszek et al. (1997). The presence of longshore crescentic forms can be seen in figure 9 which is an adaptation of the data described in Pruszek et al.'s (1997) paper. The wavelength of these crescentic forms is approximately 800 m even though the presence of only two bars and three pools does not allow a precise evaluation. By analysing the beach profile measured by Pruszek et al. (1997) during august 1996 it turns out that the values of x_w^* and h_0^* are 370 m and 2.1 m respectively. Using these input values in the theoretical model, the predicted wavelength is close to 850 m. In determining this value it has been assumed that it is caused by the maximum in the growth rate induced by the curve $\tilde{\Omega}$ versus the frequency parameter x_w . The bottom forms induced by wind waves which give rise to a maximum in $a(x_w)$ have not been observed by Pruszek et al. (1997). This may be due to the reflection coefficient of the beach. Indeed the theory predicts the appearance of crescentic forms only when the incoming waves are somewhat reflected by the beach. At Lubiatowa site the presence of a system

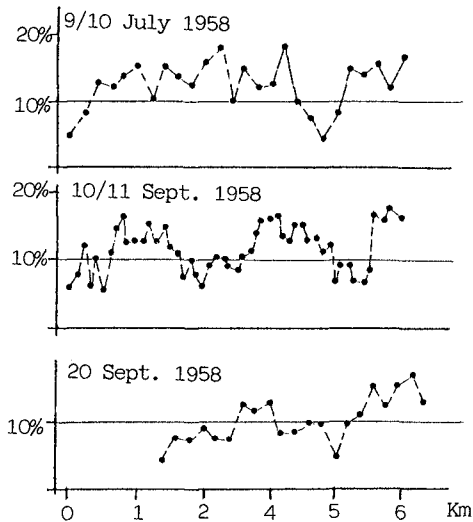


Figure 8: Shoreface slope along Tokai beach in different months of 1958 (adapted from Hom-ma & Sonu, 1963).

of longshore parallel bars induces the breaking of short waves and makes the reflection coefficient of the beach very small.

4 CONCLUSIONS

The comparison between the theoretical findings and field data described in the previous section seems to indicate that the main ingredients of the process leading to the formation of crescentic forms are captured by the simplified model formulated by Vittori et al. (1998). Of course in order to obtain more refined predictions of the characteristics of the bottom forms it would be necessary to improve the model by removing some of the assumptions introduced to work out the solution by analytical means. In particular the geometry of the beach should allow for the presence of bars and the wave model should include the description of breaking, since quite often the surf zone is not small when compared with the length of the incoming wave. Such a refined model would require a numerical approach to determine both the basic wave field and the time development of bottom perturbations.

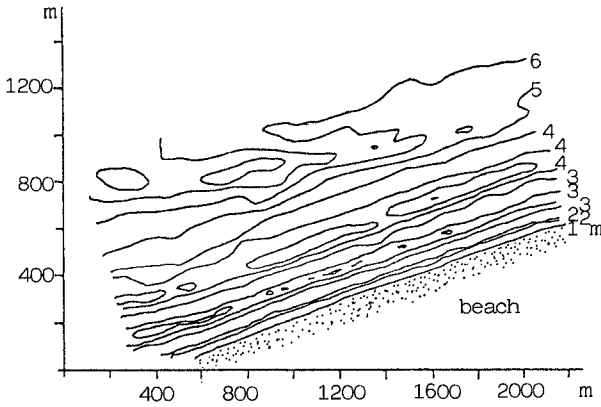


Figure 9: Bottom topography measured by Pruszk & al. (1997) at Lubiadowa beach (adapted from Pruszk et al., 1997).

Acknowledgement

This paper is partly based on work in the PACE- research project supported by EU under contract n. MAS3-CT95-0002 in the framework of the Marine Science and Technology Programme (MAST-III). The financial support of the Office of Naval Research (O.N.R.), U.S.A., under contract N. 00014-97-0790 and of the Ministero dell'Università e della Ricerca Scientifica e Tecnologica (Italy) is gratefully acknowledged.

Appendix I. References

- Abramowitz, M., and Stegun, I.A. (1964). *Handbook of mathematical functions*. Dover Publication.
- Guza R.T., and Davis, R.E. (1974). "Excitation of edge waves by waves incident on a beach". *J. Geophys. Res.*, 79(9), 1285-1291.
- Hom-ma, M., and Sonu, C. (1963). "Rhythmic pattern of longshore bars related to sediment characteristics". *8th Coastal Eng. Conference*, Mexico City, November 1962, 248-278.
- Mei, C.C. (1989). *The Applied Dynamics of Ocean Surface Waves*. World Scientific.
- Pruszk, Z., Rozynsky G., and Zeidler, R.B. (1997). "Statistical properties of multiple bars". *Coastal Eng.*, 31, 263-280.
- Vittori, G., De Swart, H.E., and Blondeaux P. (1998). "Crescentic bed forms in the nearshore region". Submitted for publication.